UTAP Journal Club on 2013/9/30

[1] Thornton, D., et al., “A Population of Fast Radio Bursts at Cosmological Distances” , arXiv:1307.1628, Science, 341, 53
[2] McQuinn, M., “Locating the "missing" baryons with extragalactic dispersion measure estimates” , arXiv:1309.4451
[3] Kaiser, N., “Measuring gravitational redshifts in galaxy clusters” , arXiv:1303.3663, MNRAS, in press
[4] Hanson, D., et al., “Detection of B-mode Polarization in the Cosmic Microwave Background with Data from the South Pole Telescope”, arXiv:1307.5830

[1]

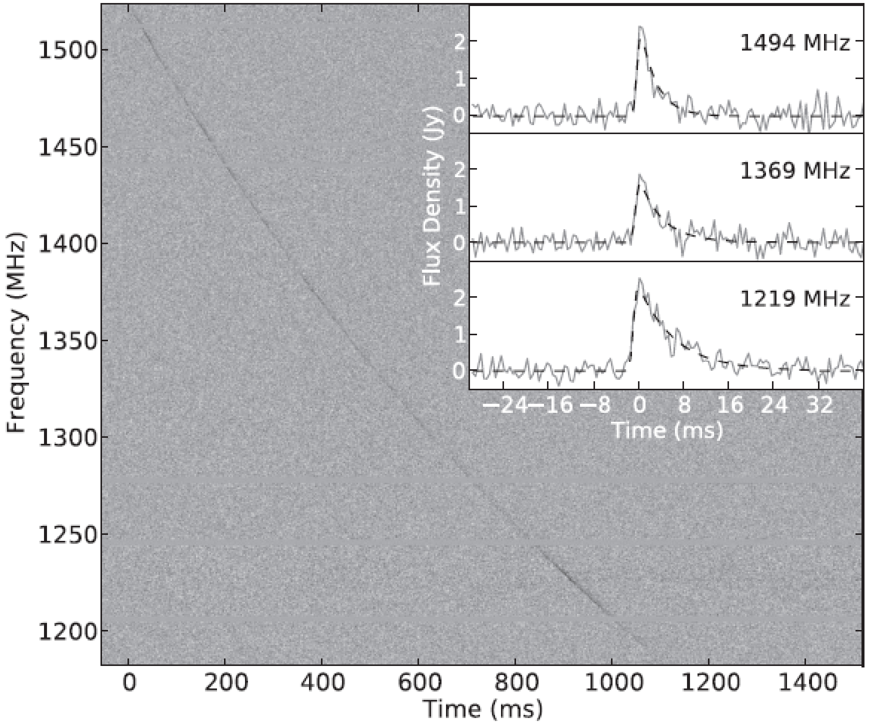

Fig. 2. A dynamic spectrum showing the frequency-dependent delay of FRB 110220. Time is measured relative to the time of arrival in the highest frequency channel. For clarity we have integrated 30 time samples, corresponding to the dispersion smearing in the lowest frequency channel. **(Inset)** The top, middle, and bottom 25-MHz-wide dedispersed subband used in the pulse-fitting analysis (*2*); the peaks of the pulses are aligned to time = 0. The data are shown as solid gray lines and the best-fit profiles by dashed black lines.

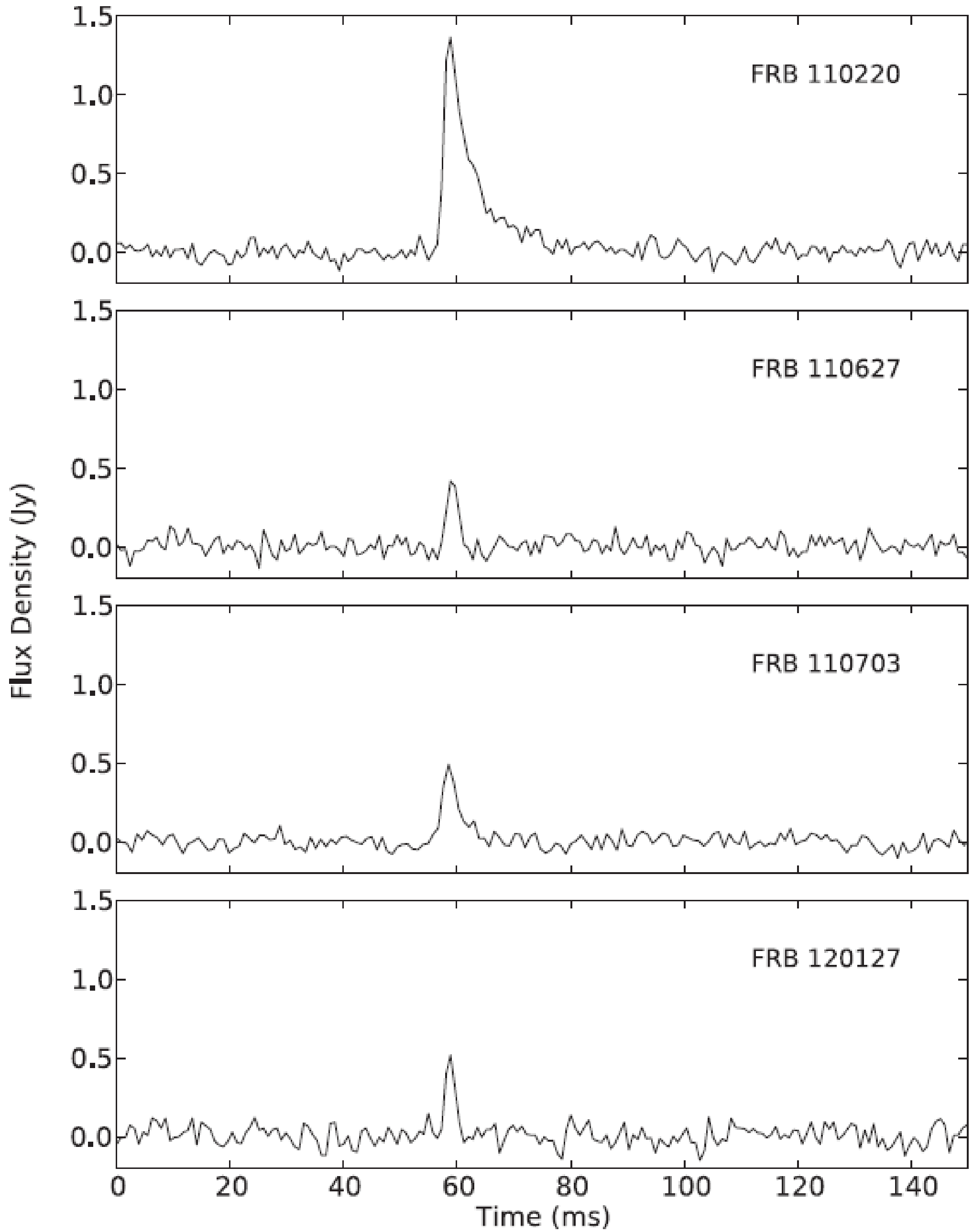

Fig. 1. The frequency-integrated flux densities for the four FRBs. The time resolutions match the level of dispersive smearing in the central frequency channel (0.8, 0.6, 0.9, and 0.5 ms, respectively).

Table 1. Parameters for the four FRBs. The position given is the center of the gain pattern of the beam in which the FRB was detected (half-power beam width ~ 14 arc min). The UTC corresponds to the arrival time at 1581.804688 MHz. The DM uncertainties depend not only on SNR but also on whether α and β are assumed ($\alpha = -2$; no scattering) or fit for; where fitted, α and β are given. The comoving distance was calculated by using DM_{Host} = 100 cm^{-3} pc (in the rest frame of the host) and a standard, flat-universe ΛCDM cosmology, which describes the expansion of the universe with baryonic and dark matter and dark energy [$H_0 = 71$ km s^{-1} Mpc^{-1}, $\Omega_M = 0.27$, $\Omega_\Lambda = 0.73$; H_0 is the Hubble constant and Ω_M and Ω_Λ are fractions of the critical density of matter and dark energy, respectively (*29*)]. α and β are from a series of fits using intrinsic pulse widths of 0.87 to 3.5 ms; the uncertainties reflect the spread of values obtained (*2*). The observed widths are shown; FRBs 110627, 110703, and 120127 are limited by the temporal resolution due to dispersion smearing. The energy released is calculated for the observing band in the rest frame of the source (*2*).

	FRB 110220	FRB 110627	FRB 110703	FRB 120127
Beam right ascension (J2000)	22^h 34^m	21^h 03^m	23^h 30^m	23^h 15^m
Beam declination (J2000)	−12° 24′	−44° 44′	−02° 52′	−18° 25′
Galactic latitude, *b* (°)	−54.7	−41.7	−59.0	−66.2
Galactic longitude, *l* (°)	+50.8	+355.8	+81.0	+49.2
UTC (dd/mm/yyyy hh:mm:ss.sss)	20/02/2011 01:55:48.957	27/06/2011 21:33:17.474	03/07/2011 18:59:40.591	27/01/2012 08:11:21.723
DM (cm^{-3} pc)	944.38 ± 0.05	723.0 ± 0.3	1103.6 ± 0.7	553.3 ± 0.3
DM_E (cm^{-3} pc)	910	677	1072	521
Redshift, *z* (DM_{Host} = 100 cm^{-3} pc)	0.81	0.61	0.96	0.45
Co-moving distance, *D* (Gpc) at *z*	2.8	2.2	3.2	1.7
Dispersion index, α	−2.003 ± 0.006	–	−2.000 ± 0.006	–
Scattering index, β	−4.0 ± 0.4	–	–	–
Observed width at 1.3 GHz, *W* (ms)	5.6 ± 0.1	<1.4	<4.3	<1.1
SNR	49	11	16	11
Minimum peak flux density S_ν (Jy)	1.3	0.4	0.5	0.5
Fluence at 1.3 GHz, *F* (Jy ms)	8.0	0.7	1.8	0.6
$S_\nu D^2$ (× 10^{12} Jy kpc^2)	10.2	1.9	5.1	1.4
Energy released, *E* (J)	~10^{33}	~10^{31}	~10^{32}	~10^{31}

[2]

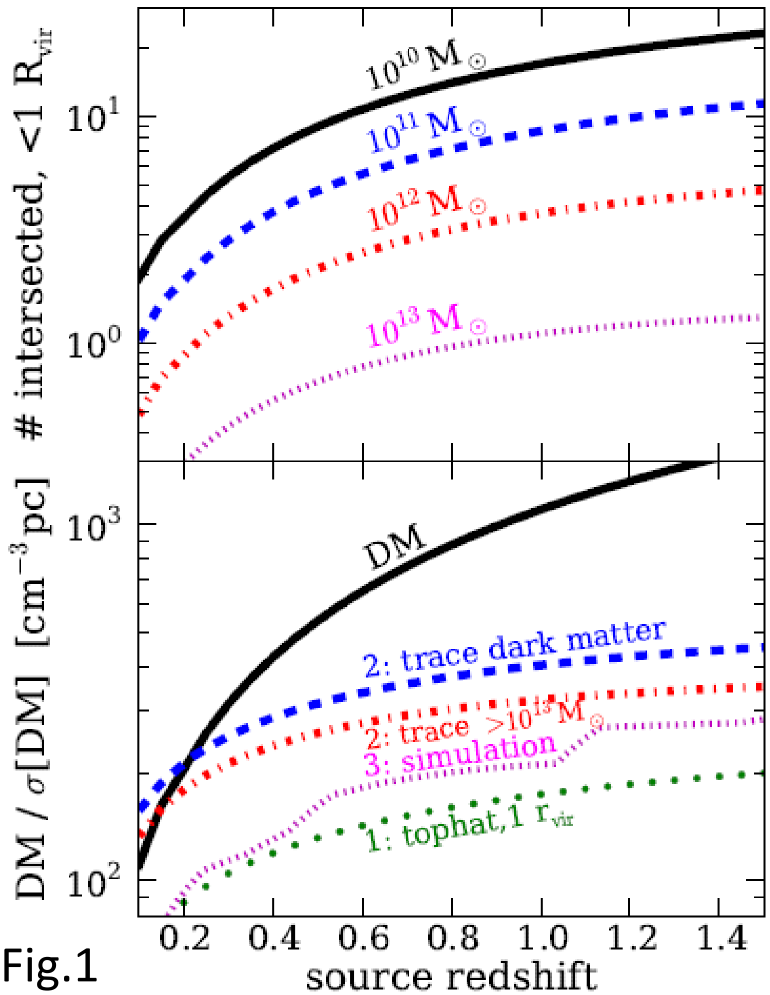

Fig.1

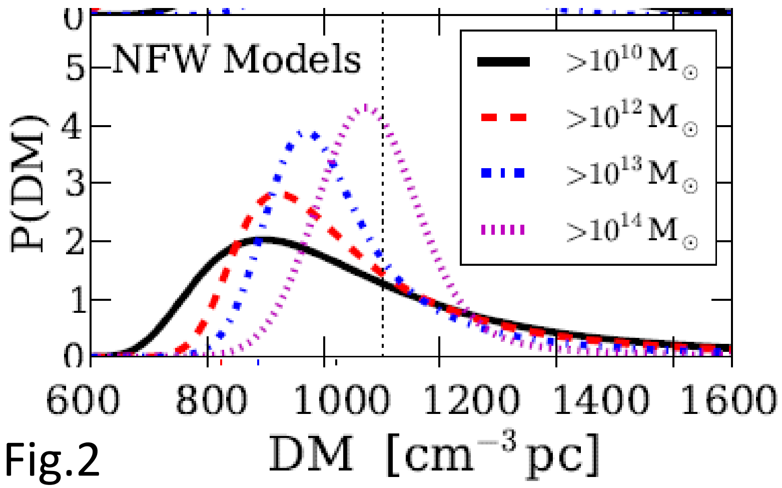

Fig.2

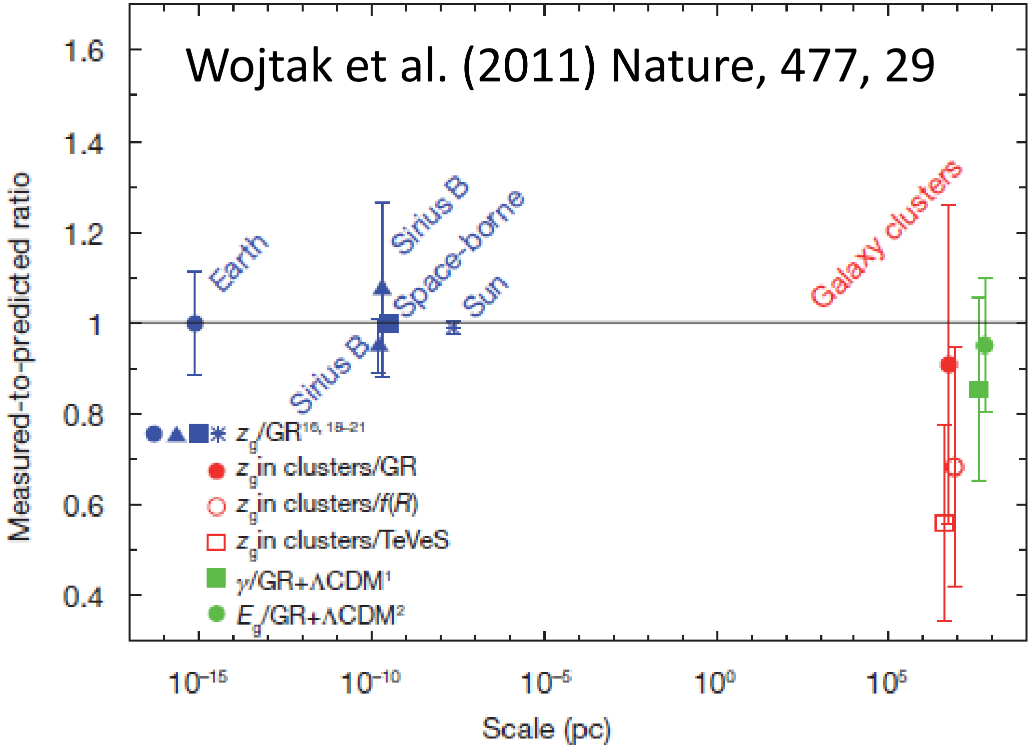

Figure 3 | The measured-to-predicted ratio of the gravitational redshift. The figure shows the results of different observations or experiments as a function of the spatial scale of the gravitational potential well. Blue and red symbols refer to detections of gravitational redshift z_g in: a ground-based experiment[16] (blue circle), observations of the Sirius B white dwarf[19,20] (blue triangles), a space-based experiment[21] (blue square), an observation of the Sun[18] (blue star), and analysis of the cluster data reported in this work (red circle). All measurements are divided by the predictions of general relativity (filled symbols). Results obtained for galaxy clusters are also compared with the predictions of $f(R)$ theory and TeVeS model (red open symbols). As a measure of gravitational redshift in galaxy clusters we used the signal integrated within the aperture of 6 Mpc. The green square and circle show the measurement of the rate of growth of cosmic structure γ (ref. 1) and the probe of gravity E_g, which combines the properties of galaxy–galaxy lensing, galaxy clustering and galaxy velocities[2]. Both results are compared with the prediction of general relativity with a standard ΛCDM cosmological model. All error bars represent standard deviations. The relative accuracy of the measurement from the space-borne experiment[21] is beyond the resolution of the plot and amounts to 10^{-4}.

[3]

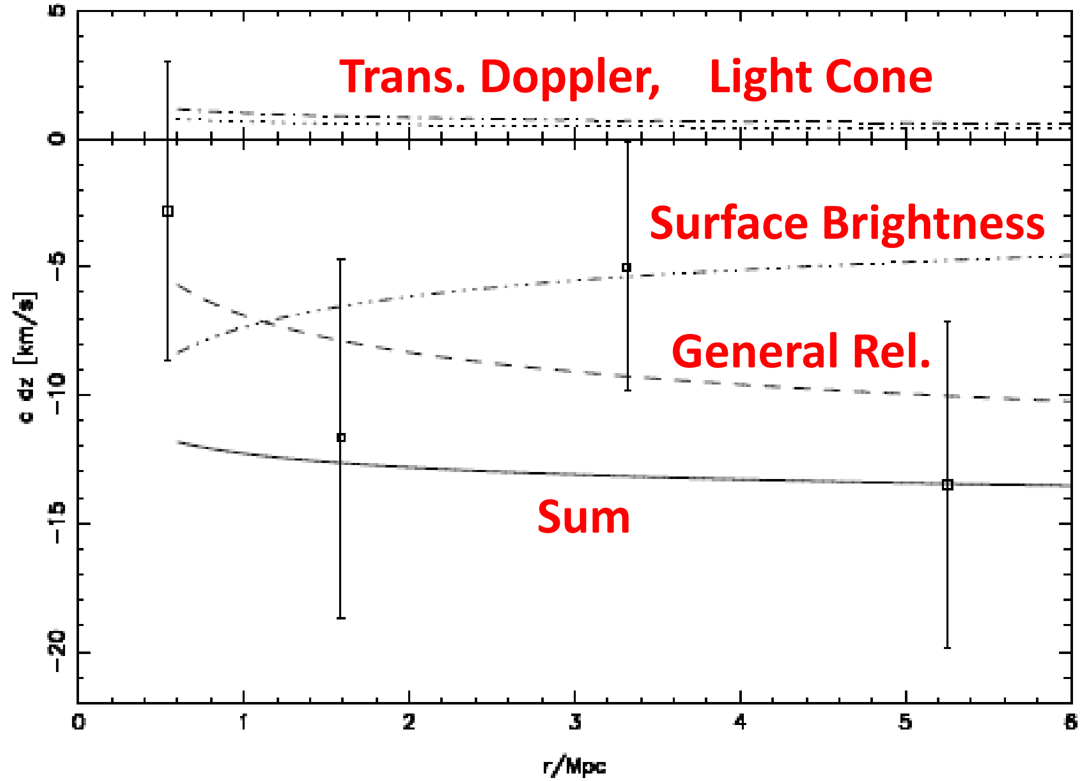

Figure 3. Data points from figure 2 of WHH and prediction based on mass-traces-light cluster halo profile and measured velocity dispersions as described in the main text. The dashed line is the gravitational redshift prediction, which is similar to the WHH model prediction. The dot-dash line is the transverse Doppler effect. The dotted line is the LC effect. The triple dot-dash line is the surface brightness effect. The solid curve is the combined effect.

[4]

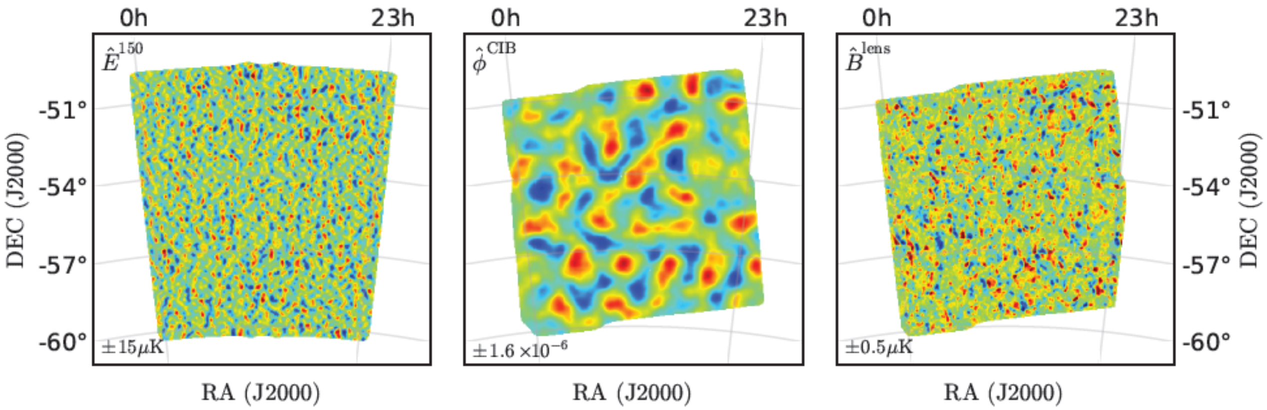

FIG. 1: (Left panel): Wiener-filtered E-mode polarization measured by SPTpol at 150 GHz. (Center panel): Wiener-filtered CMB lensing potential inferred from CIB fluctuations measured by *Herschel* at 500 μm. (Right panel): Gravitational lensing B-mode estimate synthesized using Eq. (1). The lower left corner of each panel indicates the blue(-)/red(+) color scale.

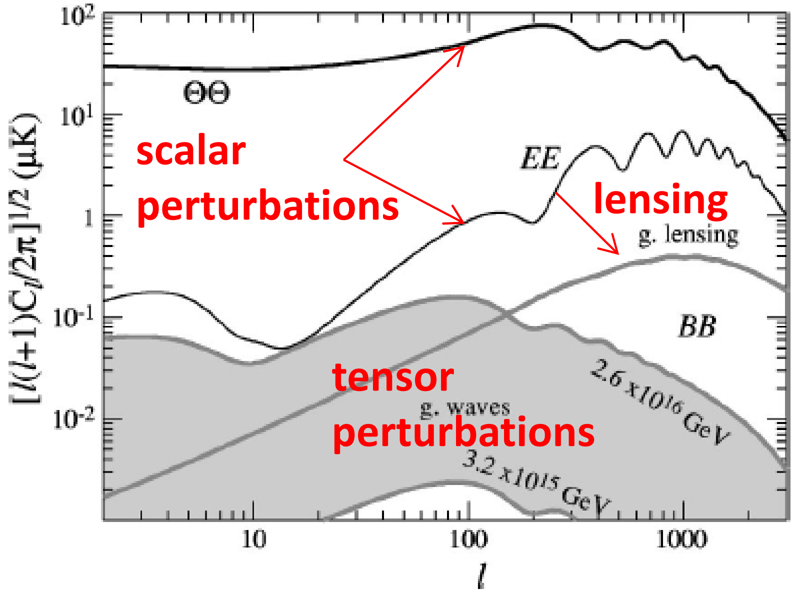

Hu et al. (2003) PRD 67, 043004

FIG. 2. Scalar CMB power spectra in temperature ($\Theta\Theta$) and E-mode polarization (EE) compared with B-mode polarization due to gravitational lensing and gravitational waves at the maximum allowable 2.6×10^{16} GeV [39] and minimum detectable 3.2×10^{15} GeV level [40] (see text). The cold dark matter model with a cosmological constant (ΛCDM) shown has parameters given in Sec. IV A.

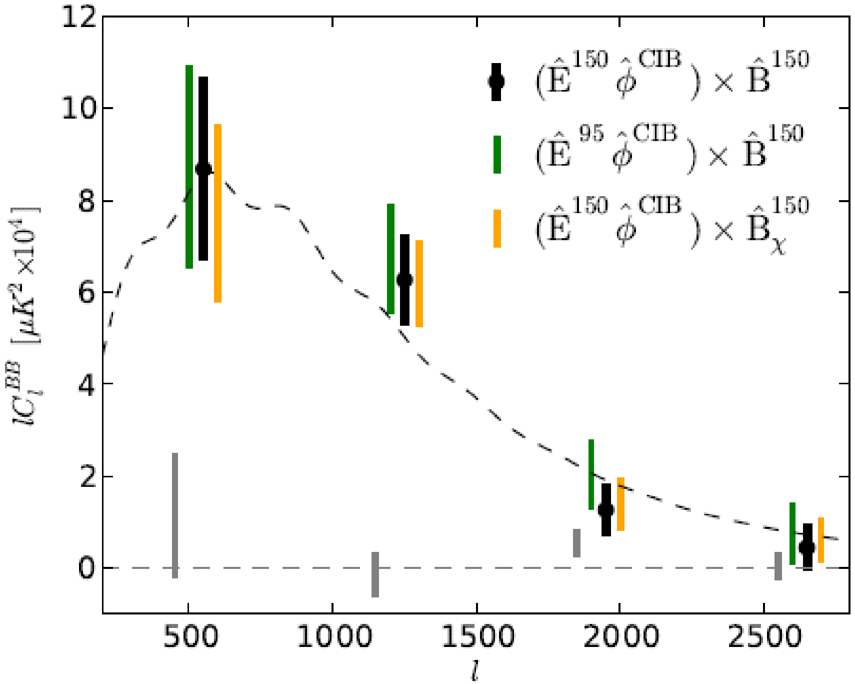

FIG. 2: (Black, center bars): Cross-correlation of the lensing B modes measured by SPTpol at 150 GHz with lensing B modes inferred from CIB fluctuations measured by *Herschel* and E modes measured by SPTpol at 150 GHz; as shown in Fig. 1. (Green, left-offset bars): Same as black, but using E modes measured at 95 GHz, testing both foreground contamination and instrumental systematics. (Orange, right-offset bars): Same as black, but with B modes obtained using the χ_B procedure described in the text rather than our fiducial Wiener filter. (Gray bars): Curl-mode null test as described in the text. (Dashed black curve): Lensing B-mode power spectrum in the fiducial cosmological model.